

Article

Fixed-Time Control of a Robotic Arm Based on Disturbance Observer Compensation

Gang Zhang ^{1,2}, Jing Pan ¹, Tianli Li ¹, Zheng Wang ³ and Duansong Wang ^{2,3,*}¹ School of Electrical Engineering, Anhui Polytechnic University, Wuhu 241000, China;

zhanggang@wxc.edu.cn (G.Z.); jingpan1102@126.com (J.P.); 2021030019@mail.wxc.edu.cn (T.L.)

² Anhui Undergrowth Crop Intelligent Equipment Engineering Research Center, Lu'an 237012, China³ School of Electrical and Photoelectronic Engineering, West Anhui University, Lu'an 237012, China; 15155538985@163.com

* Correspondence: dswangsd@126.com

Abstract: Backstepping-based fixed-time tracking control is proposed for a robotic arm system to solve the problem of trajectory tracking control under system uncertainties, which ensures the robotic arm system can realize stable tracking control within a fixed time independent of the initial state of the system. In addition, to address the uncertainties in the robotic arm system, a control strategy based on disturbance observer compensation is designed, which provides feed-forward compensation through the accurate estimation of the system uncertainties and enhances the system's robustness. Finally, a two-link robotic arm model is used for simulation experiments, and the comparison results show that the control scheme designed in this article can effectively improve the robotic arm's tracking accuracy and convergence speed.

Keywords: backstepping; robotic arm system; trajectory tracking; fixed time; disturbance observer

1. Introduction

The robotic arm, a vital component of industrial robots, has become increasingly intelligent and widely applied in industries, military, medical, aerospace, and other fields. For robotic arms, they can perform some complex tasks with human beings and work in dangerous workplaces [1]. As such, research on robotic arm control has attracted more and more experts and scholars. However, due to robotic arms being a type of complex dynamical system characterized by multivariable, nonlinear, and strongly coupled processes [2], the actual control processes of the robotic arm are affected by model errors, internal friction, external environmental disturbances, and other uncertain factors, thereby affecting the accuracy of the robotic arm trajectory tracking [3]. To achieve trajectory tracking effects with strong stability, high accuracy, and fast convergence speed, it is of practical significance to introduce control algorithms to design controllers with certain robustness for the research of robotic arm control systems [4].

In terms of robotic arm control, in order to address the complex control issues of robotic arm systems and achieve high-precision tracking performance, experts have proposed many control methods [5]. At present, the methods available for designing nonlinear control systems include sliding mode control, backstepping, robust control, model predictive control, neural network (NN) control, and adaptive control [6–9]. In ref. [6], an adaptive gain method based on state constraints was studied. This controller takes into account the influence of position and speed limitations on the trajectory tracking control of the robotic arm and conducts a comprehensive technical design for the multi-link robotic arm. The simulation results indicate that the method was superior to similar adaptive controllers that do not consider the constraints and the proportional–integral–differential form. Subsequently, a robust control law for space robots that considers system uncertainty and closed-chain constraints was proposed in ref. [7], which has the advantage of weak



Citation: Zhang, G.; Pan, J.; Li, T.; Wang, Z.; Wang, D. Fixed-Time Control of a Robotic Arm Based on Disturbance Observer Compensation. *Processes* **2024**, *12*, 93. <https://doi.org/10.3390/pr12010093>

Academic Editor: Jiaqiang E

Received: 18 November 2023

Revised: 25 December 2023

Accepted: 28 December 2023

Published: 30 December 2023



Copyright: © 2023 by the authors. Licensee MDPI, Basel, Switzerland. This article is an open access article distributed under the terms and conditions of the Creative Commons Attribution (CC BY) license (<https://creativecommons.org/licenses/by/4.0/>).

dynamic coupling in the driving system. In ref. [8], adaptive robust backstepping was proposed to enhance the performance of mobile manipulator robots; in addition, with this approach, there is no longer a need for prior knowledge of the control system, effectively improving its practicality. In ref. [9], second-order sliding mode control (SMC) based on adaptive neural networks was developed for a dual-arm robot, which can fully approximate the dynamic model of the robotic arm while ensuring the higher robustness of the entire system. It is worth noting that the above methods usually use adaptive technology to address the control problem of robotic arms, and the time required for tracking errors to reach zero is infinite.

To ensure that the tracking error of the system converges in a finite time, a finite time controller based on backstepping has been studied [10–12]. In ref. [10], an improved fault-tolerant controller was constructed by applying fuzzy control and adaptive backstepping, effectively addressing the trajectory tracking control problem of non-strict feedback nonlinear systems with actuator faults. In ref. [11], the finite-time consensus fault-tolerant control tracking problem of nonlinear multi-agent systems with non-strict feedback forms was solved by combining finite time control with neural networks and backstepping. In ref. [12], a novel control method for robotic arms based on backstepping and terminal sliding mode control was developed to address the problem of trajectory tracking control for robotic arms, which can preserve the advantages of both backstepping and sliding mode control, thus effectively improving the fast transient response and robustness of the system. Certainly, this control method can effectively accelerate the convergence velocity, and the convergence time can be given by $T \leq 1/\alpha(1 - \gamma) \ln[\alpha V^{1-\gamma}(x_0) + \beta/\beta]$. However, its convergence time is related to the initial value of the system's state, and therefore, its convergence time cannot be formulated.

In order to overcome this drawback, fixed-time theory can be exploited, ensuring a system reaches stability within a fixed timeframe; at the same time, the convergence time is independent of the system's initial state, and the convergence time can be given by $T \leq T_{max} := 1/\alpha(1 - p) + 1/\beta(q - 1)$. This method can determine the maximum convergence time of the system during the controller design process, thereby providing valuable system performance information in advance. The theory is more applicable to systems that require a strict convergence time. In ref. [13], a fault-tolerant-prescribed performance tracking control approach based on fixed-time techniques was designed to solve robot manipulators with actuator faults. By designing a fixed-time performance function with precise convergence and combining it with terminal sliding mode control, thus effectively improved the tracking accuracy of the robotic arm and the robustness of the system. To achieve fixed-time convergence and better robustness, a fixed-time sliding mode control (FTSMC) was studied in ref. [14]. By combining high-order sliding mode control and fixed time theory, the performance of the controller was effectively improved. In ref. [15], an adaptive FTSMC was also applied to robot manipulators. However, FTSMC has a drawback in that it can generate chattering effects, thereby causing mechanical oscillations in the robotic arm system. To this end, scholars have developed a fixed-time controller based on backstepping without a chattering effect or by lowering the chattering effect. In ref. [16], by combining fixed-time control, backstepping, and a newly developed obstacle function, the output tracking problem of MIMO nonlinear systems with asymmetric output constraints was successfully solved; finally, the effectiveness of the algorithm was verified through simulations using a two-degree-of-freedom robotic arm. In ref. [17], by combining fixed-time control and backstepping with a newly designed performance function, the tracking control problem for stochastic nonlinear systems with unknown measurement sensitivity was effectively solved. The widespread use of backstepping control relies on the availability of complete knowledge about robot dynamics during the design process. However, when system uncertainties are present, the tracking performance achieved by backstepping-based control strategies is often lower compared to other control methods.

In order to solve the issue of system uncertainties, scholars have proposed many effective attempts [18–25]. There are currently two main types of algorithms: (1) neural

network-based approximation algorithms; and (2) disturbance observer-based algorithms. Neural network-based algorithms can leverage their powerful approximation ability to estimate system uncertainty [18]. In ref. [19], a new fuzzy wavelet neural network (FWNN) was designed to estimate the unknown uncertainties in the presence of unknown nonlinear uncertainties by concentrating them into a composite uncertainty, thus effectively enhancing the robustness of the system. In ref. [20], a fixed-time neural network control method was studied to address system uncertainties. By integrating switching mechanisms into control design, the semi-global stability of traditional neural network control systems can be extended to global stability, effectively eliminating the impact of system uncertainties on robotic arm control. Adaptive non-singular terminal sliding mode control (NSTSMC) was developed in ref. [21], which uses neural networks to deal with system uncertainties without prior knowledge. Finally, the effectiveness of the control method was verified through simulation. Still, neural network algorithms often contain approximate residuals that can affect their accuracy, which can only achieve globally uniformly bounded tracking performance instead of asymptotic stability. In disturbance observer-based algorithms, system uncertainty is estimated by the disturbance observer. In ref. [22], a nonlinear disturbance observer is developed to address the system uncertainties of the robotic arm. Although the observer is capable of providing precise estimations of the system uncertainties, it can only achieve an asymptotically stable tracking performance, which means that the optimal convergence speed of the system is exponentially convergent, and the tracking error can converge to zero in infinite time. Subsequently, a disturbance observer based on a finite-time algorithm was proposed in ref. [23] to address the measurement uncertainties on the robotic surface vehicle (RSV).

In order to address with measurement uncertainties, two finite time disturbance observers were developed to estimate the mismatched and matched lumped disturbances in RSV kinematics and dynamics, respectively. Through feed-forward disturbance compensation, the proposed controller is not only robust to model uncertainty and environmental disturbances but also insensitive to measurement uncertainties. Although the finite-time disturbance observer can accurately estimate the disturbance on the robotic arm, its convergence time is related to the initial observation error, which limits its applicability. To our knowledge, the convergence time of fixed-time disturbance observers (FDO) is independent of the system's initial state, which has been widely used to estimate the system uncertainties of robotic arm systems in recent years. In ref. [24], a second-order sliding mode disturbance observer was designed based on fixed-time theory to enable small unmanned aerial vehicles to perform stable hovering operations, even in the presence of external interferences, compared to traditional disturbance observer-based sliding mode control methods; this control method has a faster convergence speed. In ref. [25], a uniform, robust exact differentiator was used to design a fixed-time observer, which can accurately estimate the uncertainty of the robotic arm system within a fixed timeframe. These are application examples of fixed-time disturbance observers. Currently, many scholars are studying fixed-time disturbance observers, and using fixed-time disturbance observers to solve the system uncertainty in robotic arm systems is still an open topic.

Based on the above discussion, in this article, a controller based on a fixed-time disturbance observer is proposed for the trajectory tracking control problem of n-joint robotic arms with system uncertainties. The key contributions of this research are outlined as follows:

- (1) Backstepping-based fixed-time tracking control is proposed in this article. Combining the backstepping, observer, and fixed time theory effectively improves the convergence speed and tracking precision of the robotic arm.
- (2) A fixed-time disturbance observer is designed to accurately estimate the system uncertainties existing in the robotic arm system, which provides compensation for the controller, thus improving the tracking performance and robustness of the robotic arm system. Meanwhile, we introduce the hyperbolic tangent function $\tanh(\cdot)$ to avoid the observation chattering effect.

2. Preliminaries and Problem Formulation

2.1. Preliminaries

Before the process and to make the readers easily understand the manuscript, the following lemmas are introduced.

Lemma 1 [26]. *The scalar system can be described as follows:*

$$\dot{y} = -\gamma_1 y^{2-m/n} - \gamma_2 y^{m/n}, y(0) = y_0 \quad (1)$$

where γ_1 and γ_2 are positive constants, m and n are positive odd numbers with $m < n$; thus, the system is fixed-time stable, and the upper bound on the convergence time is bounded by $T(y_0)$:

$$T(y_0) \leq \frac{n\pi}{2\sqrt{\gamma_1\gamma_2}(n-m)} \quad (2)$$

Lemma 2 [27]. *There exists a continuous radially unbounded function $V: \mathbb{R}^n \rightarrow \mathbb{R}_+ \cup 0$, which satisfies:*

- (1) $V(\mu) = 0 \Leftrightarrow \mu = 0$
- (2) *If the solution $\mu(t)$ satisfies the inequality as follows:*

$$V(\mu) \leq -\alpha V^p(\mu) - \beta V^q(\mu) \quad (3)$$

where α , β , p , and q are positive constants, $0 < p < 1$, $q > 1$. Then, the system is globally fixed-time stable with settling time T satisfying

$$T \leq T_{max} := \frac{1}{\alpha(1-p)} + \frac{1}{\beta(q-1)} \quad (4)$$

Remark 1. *From (4), we know that the convergence time of the system is only related to system parameters α , β , p and q , and it is not related to the initial state of the system. In real-world applications in engineering, this algorithm is more suitable when there are strict requirements for the convergence time.*

Lemma 3 [28]. *There exists a continuous radially bounded function $V: \mathbb{R}^n \rightarrow \mathbb{R}_+ \cup 0$, which satisfies:*

- (1) $V(\mu) = 0 \Leftrightarrow \mu = 0$
- (2) *If the solution $\mu(t)$ satisfies the inequality as follows:*

$$V(\mu) \leq -\alpha V^p(\mu) - \beta V^q(\mu) + \vartheta \quad (5)$$

where α , β , p , q , and ϑ are positive constants, $0 < p < 1$, $q > 1$. Then, the system is actually fixed-time stable with a settling time T satisfying

$$T \leq T_{max} := \frac{1}{\alpha\theta(1-p)} + \frac{1}{\beta\theta(q-1)} \quad (6)$$

where $0 < \theta < 1$.

Lemma 4 [29]. *If $t_1, t_2, \dots, t_M \geq 0$, we have*

$$\begin{cases} \sum_{i=1}^M t_i^k \geq \left(\sum_{i=1}^M t_i\right)^k & 0 < k \leq 1 \\ \sum_{i=1}^M t_i^k \geq M^{1-k} \left(\sum_{i=1}^M t_i\right)^k & 1 < k < \infty \end{cases} \quad (7)$$

2.2. Problem Formulation

The dynamics of a n-link robotic arm is as follows [30]:

$$M(q)\ddot{q} + C(q, \dot{q})\dot{q} + G(q) = \tau(t) - J^T(q)f(t) \quad (8)$$

where $q \in R^n$ represents the position vector, and $\dot{q} \in R^n$ and $\ddot{q} \in R^n$ represent the speed and acceleration vectors, respectively. $M(q) \in R^{n \times n}$ is the symmetric positive definite inertia matrix with the property $M(q) = M^T(q)$. $C(q, \dot{q}) \in R^{n \times n}$ is the Coriolis–centripetal matrix, and $G(q) \in R^n$ denotes the gravitational matrix. $\tau(t) \in R^n$ is the control input of the system. $J(q)$ means the Jacobian matrix. $f(t) \in R^n$ denotes the vector of the constrained force exerted by the user and the environment.

To facilitate the control design, let

$$\begin{cases} x = q \\ v = \dot{q} \end{cases} \quad (9)$$

Then, according to Equations (8) and (9), the robotic arm dynamics can be rewritten as follows:

$$\begin{cases} \dot{x} = v \\ \dot{v} = M^{-1}(x)[\tau(t) - C(x, v)v - G(x)] + \omega \end{cases} \quad (10)$$

where $\omega = -M^{-1}(x)J^T(x)f(t)$ represents the system uncertainties.

According to Equation (10), the tracking trajectory can be described as follows:

$$\begin{cases} \dot{x}_d = v_d \\ \dot{v}_d = M_d^{-1}(x)[\tau_d(t) - C(x_d, v_d)v_d - G(x_d)] \end{cases} \quad (11)$$

where $x_d = [q_{d1} \ q_{d2} \ \dots \ q_{dn}]^T$ and $v_d = [\dot{q}_{d1} \ \dot{q}_{d2} \ \dots \ \dot{q}_{dn}]^T$ denote the desired position vector and velocity vector of the robotic arm, respectively, and $\tau_d(t) - C(x_d, v_d)v_d - G(x_d)$ is the desired dynamics.

In order to achieve the design of subsequent control strategies, we propose the following assumption.

Assumption 1. The constrained force $f(t)$ is bounded, such that there exists a constant $L > 0$, which satisfies $\|\omega\| \leq L \leq +\infty$, where $\|\cdot\|$ represents the 2-norm of the matrix or vector.

Remark 2. This assumption is reasonable. From an engineering perspective, the time-varying constrained force $f(t)$ is bounded due to the physical structure limitation.

The main control objectives of this paper are to design a disturbance observer-based trajectory tracking control law for a robotic arm under Assumption 1 so that the robotic arm can track the desired trajectory while ensuring that all signals in the closed-loop system are globally fixed-time stable. The mathematical form is described as follows:

$$\lim_{t \rightarrow T} \|x - x_d\| = 0 \quad (12)$$

where T is a positive constant, which is the expected convergence time, and $T \in [0, +\infty)$.

3. Controller Design without System Uncertainties

The controller without system uncertainties can be designed as follows:

Step 1: Define the position error $e_1 \in R^n$ between the actual position and the desired trajectory of the robotic arm as follows:

$$e_1 = x - x_d \quad (13)$$

According to Equations (10) and (11), the derivative of Equation (13) is:

$$\dot{e}_1 = v - v_d \quad (14)$$

Select the kinematic controller α_v as follows:

$$\alpha_v = v_d - \alpha e_1^{2-m/n} - \beta e_1^{m/n} - k_0 e_1 \quad (15)$$

where α , β and k_0 are positive constants, and m and n are positive odd numbers with $m < n$. Consider the Lyapunov function as follows:

$$V_1 = \frac{1}{2} e_1^T e_1 \quad (16)$$

The time derivative of V_1 is:

$$\begin{aligned} \dot{V}_1 &= e_1^T \dot{e}_1 \\ &= e_1^T (v - v_d) \\ &= e_1^T (-\alpha e_1^{2-m/n} - \beta e_1^{m/n} - k_0 e_1) \\ &= -\alpha e_1^{3-m/n} - \beta e_1^{1+m/n} - k_0 e_1^2 \\ &= -k_0 e_1^2 - \alpha \times 2^{\frac{3-m/n}{2}} \times \left(\frac{1}{2} e_1^2\right)^{\frac{3-m/n}{2}} - \beta \times 2^{\frac{1+m/n}{2}} \left(\frac{1}{2} e_1^2\right)^{\frac{1+m/n}{2}} \\ &\leq -\alpha \times 2^{\frac{3n-m}{2n}} V_1^{2-\frac{m+n}{2n}} - \beta \times 2^{\frac{m+n}{2n}} V_1^{\frac{m+n}{2n}} \\ &= -\lambda_1 V_1^{2-p/q} - \lambda_2 V_1^{p/q} \end{aligned} \quad (17)$$

where $\lambda_1 = \alpha \times 2^{\frac{3n-m}{2n}}$, $\lambda_2 = \beta \times 2^{\frac{m+n}{2n}}$, $p = m + n$, $q = 2n$ and $p < q$.

Combined with Lemma 1, the position tracking error e_1 is able to achieve stability at a fixed time, and the convergence time T_1 can be calculated by:

$$T_1 = \frac{q\pi}{2\sqrt{\lambda_1\lambda_2}(q-p)} \quad (18)$$

Step 2: Define the speed error $e_2 \in R^n$ as follows:

$$e_2 = v - \alpha_v \quad (19)$$

According to Equation (10), we further have:

$$\dot{e}_2 = M^{-1}[\tau(t) - C(x, v)v - G(x)] - \dot{\alpha}_v \quad (20)$$

The control strategy $\tau(t)$ can be designed as follows:

$$\tau(t) = M[-k_1 e_2 - \alpha e_2^{2-m/n} - \beta e_2^{m/n} + \dot{\alpha}_v] + C(x, v)v + G(x) \quad (21)$$

where $k_1 > 0$.

Substituting Equation (21) into Equation (20) yields:

$$\dot{e}_2 = -k_1 e_2 - \alpha e_2^{2-m/n} - \beta e_2^{m/n} \quad (22)$$

Consider the Lyapunov function as follows:

$$V_2 = \frac{1}{2} e_2^T e_2 \quad (23)$$

The time derivative of V_2 is as follows:

$$\begin{aligned}\dot{V}_2 &= e_2^T \dot{e}_2 \\ &= e_2^T \left(-k_1 e_2 - \alpha e_2^{2-m/n} - \beta e_2^{m/n} \right) \\ &= -k_1 e_2^2 - \alpha e_2^{3-m/n} - \beta e_2^{1+m/n} \\ &\leq -\alpha \times 2^{\frac{3n-m}{2n}} V_2^{\frac{3n-m}{2n}} - \beta \times 2^{\frac{m+n}{2n}} V_2^{\frac{m+n}{2n}} \\ &= -\lambda_3 V_2^{2-\frac{p}{q}} - \lambda_4 V_2^{\frac{p}{q}}\end{aligned}\quad (24)$$

where $\lambda_3 = \alpha \times 2^{\frac{3n-m}{2n}}$, $\lambda_4 = \beta \times 2^{\frac{m+n}{2n}}$, $p = m + n$, $q = 2n$ and $p < q$.

According to Lemma 1, the speed tracking error e_2 can reach zero, and the convergence time of T_2 is calculated as follows:

$$T_2 = \frac{q\pi}{2\sqrt{\lambda_3\lambda_4}(q-p)} \quad (25)$$

Theorem 1. *The B-FTTC strategy (21) designed in this article enables the robotic arm to track the desired trajectory within a fixed time T_3 , and the convergence time is independent of the system's initial state.*

Proof. Select the following Lyapunov function:

$$\begin{aligned}V_3 &= V_1 + V_2 \\ &= \frac{1}{2}e_1^T e_1 + \frac{1}{2}e_2^T e_2\end{aligned}\quad (26)$$

Take the time derivative of V_3 as follows:

$$\begin{aligned}\dot{V}_3 &= e_1^T (\dot{v} - \dot{v}_d) + e_2^T \left(-k_1 e_2 - \alpha e_2^{2-m/n} - \beta e_2^{m/n} \right) \\ &= e_1^T \left(-\alpha e_1^{2-m/n} - \beta e_1^{m/n} - k_0 e_1 \right) + e_2^T \left(-k_1 e_2 - \alpha e_2^{2-m/n} - \beta e_2^{m/n} \right) \\ &= -\alpha e_1^{3-m/n} - \beta e_1^{1+m/n} - k_0 e_1^2 - k_1 e_2^2 - \alpha e_2^{3-m/n} - \beta e_2^{1+m/n} \\ &= -k_0 e_1^2 - k_1 e_2^2 - \alpha \left(e_1^{3-m/n} + e_2^{3-m/n} \right) - \beta \left(e_1^{1+m/n} + e_2^{1+m/n} \right) \\ &\leq -\alpha \times 2^{\frac{3n-m}{2n}} \left[\left(\frac{1}{2} e_1^2 \right)^{\frac{3n-m}{2n}} + \left(\frac{1}{2} e_2^2 \right)^{\frac{3n-m}{2n}} \right] - \beta \times 2^{\frac{m+n}{2n}} \left[\left(\frac{1}{2} e_1^2 \right)^{\frac{m+n}{2n}} + \left(\frac{1}{2} e_2^2 \right)^{\frac{m+n}{2n}} \right]\end{aligned}\quad (27)$$

According to Lemma 4, we further have:

$$\begin{aligned}\dot{V}_3 &\leq -2\alpha \times V_3^{\frac{3n-m}{2n}} - \beta \times 2^{\frac{m+n}{2n}} V_3^{\frac{m+n}{2n}} \\ &= -\lambda_5 V_3^v - \lambda_6 V_3^\sigma\end{aligned}\quad (28)$$

where $\lambda_5 = 2\alpha$, $\lambda_6 = \beta \times 2^{\frac{m+n}{2n}}$, $v = \frac{3n-m}{2n}$, $\sigma = \frac{m+n}{2n}$, $\lambda_5 > 0$, $\lambda_6 > 0$, $v > 1$ and $0 < \sigma < 1$.

Combined with Lemma 2, this control system is globally fixed-time stable, and the convergence time T_3 can be calculated by:

$$\begin{aligned}T_3 \leq T_{\max} &= \frac{1}{\lambda_5(v-1)} + \frac{1}{\lambda_6(1-\sigma)} \\ &= \frac{n}{n-m} \left(\frac{1}{\alpha} + \frac{2^{\frac{n-m}{2n}}}{\beta} \right)\end{aligned}\quad (29)$$

It follows that the B-FTTC strategy designed in this section enables the robotic arm to track the desired trajectory within a fixed time.

That brings an end to the proof. \square

4. Controller Design with System Uncertainties

4.1. Disturbance Observer Design

There are system uncertainties in the actual control system of the robotic arm, and the entire system's control accuracy is affected. In order to mitigate the influence of system uncertainties on the system, the dynamic model of the mechanical arm is combined with a disturbance observer. We can use disturbance observers to estimate the system uncertainties accurately. By correcting the estimated value of the system uncertainties, the error between the actual value and the estimated value of the system uncertainties can reach zero. The following is the specific design process.

Step 1: Define an auxiliary variable:

$$E = v - \Gamma \quad (30)$$

where Γ is given by:

$$\begin{cases} \dot{\Gamma} = M^{-1}(\tau(t) - C(x, v)v - G(x)) + \hat{\omega} \\ \hat{\omega} = \kappa_1 E + \kappa_2 E^{\alpha_1} + \kappa_3 E^{\beta_1} + \kappa_4 \tanh(E) \end{cases} \quad (31)$$

where $\kappa_i \in R^{2 \times 2} (i = 1, 2, 3, 4)$ is a positive definite diagonal matrix and each element in κ_4 is greater than L , α_1 and β_1 are positive constants with $0 < \alpha_1 < 1$ and $\beta_1 > 1$, $\tanh(\cdot)$ is the hyperbolic tangent function, and $\hat{\omega}$ is the estimation of ω .

According to Equations (10) and (31), the derivative of Equation (30) is as follows:

$$\begin{aligned} \dot{E} &= \dot{v} - \dot{\Gamma} \\ &= M^{-1}(x)(\tau(t) - C(x, v)v - G(x)) + \omega - M^{-1}(\tau(t) - C(x, v)v - G(x)) - \hat{\omega} \\ &= \omega - \kappa_1 E - \kappa_2 E^{\alpha_1} - \kappa_3 E^{\beta_1} - \kappa_4 \tanh(E) \end{aligned} \quad (32)$$

Step 2: Define the observation error $\tilde{\omega}$ as follows:

$$\tilde{\omega} = \hat{\omega} - \omega \quad (33)$$

From (31) to (32), we have

$$\begin{aligned} \tilde{\omega} &= \hat{\omega} - \omega \\ &= \kappa_1 E + \kappa_2 E^{\alpha_1} + \kappa_3 E^{\beta_1} + \kappa_4 \tanh(E) - \dot{E} - \kappa_1 E - \kappa_2 E^{\alpha_1} - \kappa_3 E^{\beta_1} - \kappa_4 \tanh(E) \\ &= -\dot{E} \end{aligned} \quad (34)$$

According to Equation (34), we know that if \dot{E} converges, then $\tilde{\omega}$ also converges.

Theorem 2. Under Assumption 1, the disturbance observer in (31) can accurately estimate the ω within a fixed time with an estimation error of zero.

Proof. Select the following Lyapunov function:

$$V_4 = \frac{1}{2} E^T E \quad (35)$$

According to Equation (32), taking the time derivative of V_4 yields:

$$\begin{aligned} \dot{V}_4 &= E^T \dot{E} \\ &= E^T (\omega - \kappa_1 E - \kappa_2 E^{\alpha_1} - \kappa_3 E^{\beta_1} - \kappa_4 \tanh(E)) \\ &\leq -\kappa_2 (E^T E)^{\frac{\alpha_1+1}{2}} - \kappa_3 (E^T E)^{\frac{\beta_1+1}{2}} - L E^T \tanh(E) + L \|E\| \\ &\leq -\hat{\lambda}_{\min}(\kappa_2) (E^T E)^{\frac{\alpha_1+1}{2}} - \hat{\lambda}_{\min}(\kappa_3) (E^T E)^{\frac{\beta_1+1}{2}} + L \delta_1 \\ &= -2^{\frac{\alpha_1+1}{2}} \hat{\lambda}_{\min}(\kappa_2) V_4^{\frac{\alpha_1+1}{2}} - 2^{\frac{\beta_1+1}{2}} \hat{\lambda}_{\min}(\kappa_3) V_4^{\frac{\beta_1+1}{2}} + \vartheta \end{aligned} \quad (36)$$

where $\vartheta = L\delta_1$, and δ_1 is a positive constant.

Combined with Lemma 3, the system is actually fixed-time stable with a settling time T_4 satisfying:

$$T_4 \leq \frac{2^{\frac{1-\alpha_1}{2}}}{\tilde{\lambda}_{\min}(\kappa_2)\theta(1-\alpha_1)} + \frac{2^{\frac{1-\beta_1}{2}}}{\tilde{\lambda}_{\min}(\kappa_3)\theta(\beta_1-1)} \tag{37}$$

According to the definition of V_4 , when $t \geq T_4$, we have $V_4 \equiv 0$, $\dot{V}_4 \equiv 0$ and $\dot{E} = 0$, and we further have $\tilde{\omega} = 0$.

This brings an end to the proof. \square

Remark 3. Compared with traditional disturbance observers, the observer proposed in this paper can achieve an accurate estimation of system uncertainties while ensuring that the observation error can converge to zero within a fixed time, and that the convergence time is independent of the initial observation error. At the same time, it can effectively avoid the problem of observation chattering.

4.2. Controller Design

A diagram of the robotic arm tracking control was shown in Figure 1. The control strategy for the robotic arm system was designed as follows:

$$\tau(t) = M[-k_1e_2 - \alpha e_2^{2-m/n} - \beta e_2^{m/n} + \dot{\alpha}_v - \tilde{\omega}] + C(x, v)v + G(x) \tag{38}$$

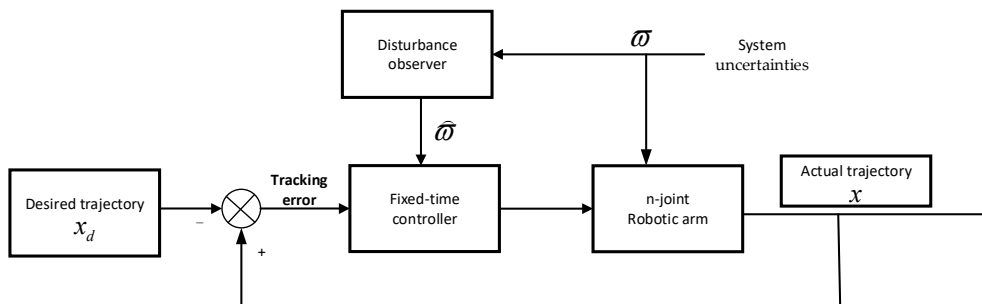


Figure 1. A diagram of the robotic arm tracking control.

Theorem 3. Under system uncertainties, the control strategy in (38) enables the robotic arm to track the desired trajectory within a fixed time T_5 .

Proof. The time derivative of V_3 can be rewritten as follows:

$$\begin{aligned} \dot{V}_3 &= e_1^T \dot{e}_1 + e_2^T \dot{e}_2 \\ &= e_2^T (\omega - \hat{\omega}) - \alpha e_1^{3-m/n} - \beta e_1^{1+m/n} - k_0 e_1^2 - k_1 e_2^2 - \alpha e_2^{3-m/n} - \beta e_2^{1+m/n} \end{aligned} \tag{39}$$

Under the action of an observer, the observing error $\tilde{\omega} = \hat{\omega} - \omega = 0, t \geq T_4$ and \dot{V}_3 would be reformulated as follows:

$$\begin{aligned} \dot{V}_3 &= -\alpha e_1^{3-m/n} - \beta e_1^{1+m/n} - k_0 e_1^2 - k_1 e_2^2 - \alpha e_2^{3-m/n} - \beta e_2^{1+m/n} \\ &= -k_0 e_1^2 - k_1 e_2^2 - \alpha \left(e_1^{3-m/n} + e_2^{3-m/n} \right) - \beta \left(e_1^{1+m/n} + e_2^{1+m/n} \right) \\ &\leq -\alpha \times 2^{\frac{3n-m}{2n}} \left[\left(\frac{1}{2} e_1^2 \right)^{\frac{3n-m}{2n}} + \left(\frac{1}{2} e_2^2 \right)^{\frac{3n-m}{2n}} \right] - \beta \times 2^{\frac{m+n}{2n}} \left[\left(\frac{1}{2} e_1^2 \right)^{\frac{m+n}{2n}} + \left(\frac{1}{2} e_2^2 \right)^{\frac{m+n}{2n}} \right] \\ &\leq -2\alpha \times V_3^{\frac{3n-m}{2n}} - \beta \times 2^{\frac{m+n}{2n}} V_3^{\frac{m+n}{2n}} \\ &= -\lambda_5 V_3^v - \lambda_6 V_3^\sigma \end{aligned} \tag{40}$$

where $\lambda_5 = 2\alpha, \lambda_6 = \beta \times 2^{\frac{m+n}{2n}}, v = \frac{3n-m}{2n}, \sigma = \frac{m+n}{2n}, \lambda_5 > 0, \lambda_6 > 0, v > 1$ and $0 < \sigma < 1$.

Combined with Lemma 2, this control system is globally fixed-time stable, and the settling time is $T_5 \leq T_3 + T_4$.

This brings an end to the proof. \square

5. Simulation Verification

In this section, to verify the effectiveness of the proposed method, we will use two cases to verify the effectiveness of the proposed method:

Case 1: Verify the control method proposed in this article with different initial conditions.

Case 2: Compare with the control method proposed in ref. [21] to verify the effectiveness of the control method proposed in this article.

The planar model of a two-link rehabilitation robot [21] is given in Figure 2.

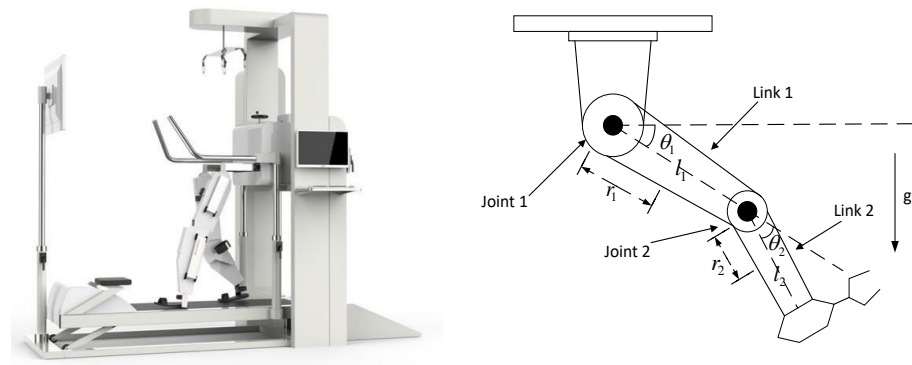


Figure 2. Planar model of the two-link rehabilitation robot. Where l_i and m_i denote the length and mass of the link i , respectively. r_i represents the distance from the joint $i - 1$ to the center of mass of the link i , where $i = 1, 2$.

Define:

$$q = \begin{bmatrix} q_1 \\ q_2 \end{bmatrix} = \begin{bmatrix} \theta_1 \\ \theta_2 \end{bmatrix} \quad (41)$$

According to ref. [30], we can use the Euler–Lagrange equation to express the dynamics of the rehabilitation robot as Equation (8), where:

$$M(q) = \begin{bmatrix} m_1 r_1^2 + m_2 (l_1^2 + r_2^2 + 2l_1 r_2 \cos(q_2)) + I_1 + I_2 & m_2 (r_2^2 + l_1 r_2 \cos(q_2)) + I_2 \\ m_2 (r_2^2 + l_1 r_2 \cos(q_2)) + I_2 & m_2 r_2^2 + I_2 \end{bmatrix} \quad (42)$$

$$C(q, \dot{q}) = \begin{bmatrix} -m_2 l_1 r_2 \dot{q}_2 \sin(q_2) & -m_2 l_1 r_2 (\dot{q}_1 + \dot{q}_2) \sin(q_2) \\ m_2 l_1 r_2 \dot{q}_1 \sin(q_2) & 0 \end{bmatrix} \quad (43)$$

$$G(q) = \begin{bmatrix} (m_1 r_2 + m_2 l_1) g \cos(q_1) + m_2 r_2 g \cos(q_1 + q_2) \\ m_2 r_2 g \cos(q_1 + q_2) \end{bmatrix} \quad (44)$$

$$J(q) = \begin{bmatrix} -(l_1 \sin(q_1) + l_2 \sin(q_1 + q_2)) & -l_2 \sin(q_1 + q_2) \\ l_1 \cos(q_1) + l_2 \cos(q_1 + q_2) & l_2 \cos(q_1 + q_2) \end{bmatrix} \quad (45)$$

The parameters of the robotic arm are shown in Table 1.

In order to validate the proposed control scheme in this article, we used MATLAB R2018b for simulations and the processor of the computer was an Intel(R), Core(TM), i7-8550U, CPU @ 1.80 GHz, 1.99 GHz. We conducted simulations using the aforementioned model, and the initial conditions were set as follows:

$$\begin{cases} q_1(0) = q_2(0) = 0.2 \\ \dot{q}_1(0) = \dot{q}_2(0) = 0 \end{cases} \quad (46)$$

Table 1. The parameters of the robotic arm.

Parameter	Description	Value
m_1	Mass of link 1	2.00 kg
m_2	Mass of link 2	0.85 kg
l_1	Length of link 1	0.35 m
l_2	Length of link 2	0.31 m
I_1	Moment of inertia of link 1	0.06125 kgm ²
I_2	Moment of inertia of link 2	0.02042125 kgm ²

The controller and observer parameters were set as follows: $k_0 = 0.5, k_1 = 15, \alpha = 20, \beta = 5, m = 9, n = 13, \kappa_1 = \begin{bmatrix} 35 & 0 \\ 0 & 35 \end{bmatrix}, \kappa_2 = \begin{bmatrix} 4 & 0 \\ 0 & 4 \end{bmatrix}, \kappa_3 = \begin{bmatrix} 5 & 0 \\ 0 & 5 \end{bmatrix}, \kappa_4 = \begin{bmatrix} 100 & 0 \\ 0 & 1000 \end{bmatrix}, \alpha_1 = 0.6, \text{ and } \beta_1 = 2$. The simulation time was set for 40 s, and the value of the constrained force vector was assumed as $f(t) = [0.2 \sin(t) \quad 0.2 \cos(t)]^T$.

Case 1: compared with different initial states in the proposed method.

To verify that the convergence time of the system is independent of the initial state with the designed control law, the algorithm proposed in this article was validated with different initial states, $q(0) = [0.2 \quad 0.2]^T, q(0) = [0.4 \quad 0.4]^T$ and $q(0) = [0.6 \quad 0.6]^T$, and the simulation results are shown in Figures 3 and 4.

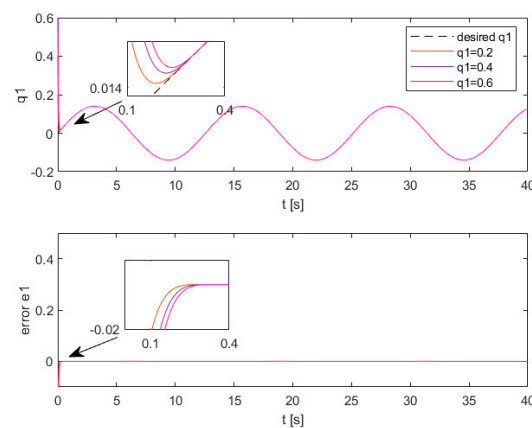


Figure 3. The trajectory tracking and error of joint 1 with different initial states.

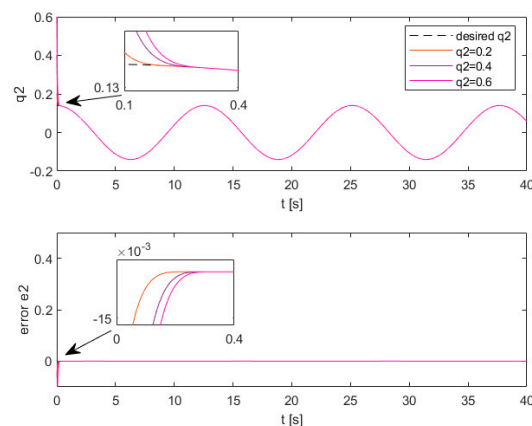


Figure 4. The trajectory tracking and error of joint 2 with different initial states.

The simulation results in Figures 3 and 4 validate the correctness and effectiveness of the designed control algorithm. With different initial states, the controller achieved system stability and control objectives within a fixed time.

Case 2: compared with ref. [21].

The controller designed in ref. [21] is as follows:

$$\begin{aligned} \dot{\tau} = & M \ddot{x}_d + Mk_1\dot{x}_d - M(\dot{Q} + k_1M^{-1})\tau \\ & + \hat{W}^T Z - \frac{b}{a}Mk_3^{-1}\dot{s}_1^{2-a/b} \\ & - \frac{bg}{ah}Mk_3^{-1}k_2 \text{diag}(|s_1|^{g/h-1})\dot{s}_1^{2-a/b} \\ & - M(k_4s_2 + k_5\text{sgn}^{2l-1}(s_2)) \end{aligned} \quad (47)$$

The controller parameters are set as follows:

$$k_1 = \text{diag}[100, 5], k_2 = \text{diag}[0.001, 0.001], k_3 = \text{diag}[0.15, 0.15], k_4 = \text{diag}[50, 50], \\ a = 0.9, b = 0.5, g = 0.6, h = 0.2, \Gamma_1 = 10I_{16 \times 16}, \Gamma_2 = 10I_{16 \times 16}.$$

In order to demonstrate the efficacy of the designed controller, a comparative analysis was performed with the adaptive non-singular terminal sliding mode control (NSTSMC) proposed in [21]. Figures 5–9 show the simulation results of the experiment.

The trajectory tracking and error of joints 1 and 2 are shown in Figures 5 and 6, where q_1 and q_{d1} represent the actual motion trajectory and desired motion trajectory of joint 1 of the robotic arm, respectively, and q_2 and q_{d2} represent the actual motion trajectory and desired motion trajectory of joint 2 of the robotic arm, respectively. By analyzing Figures 5 and 6, it is evident that the control method proposed in this article exhibits higher accuracy in tracking errors e_1 and e_2 compared to the NSTSMC.

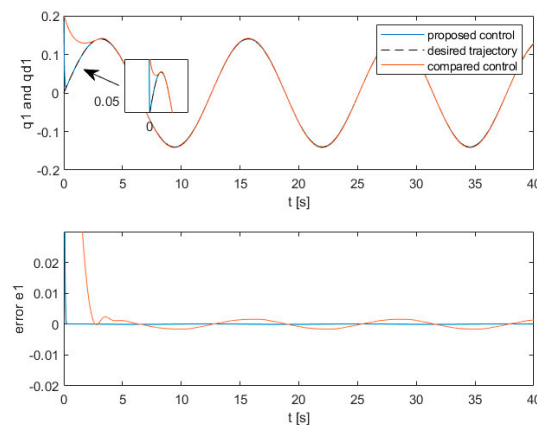


Figure 5. The trajectory tracking and error of joint 1.

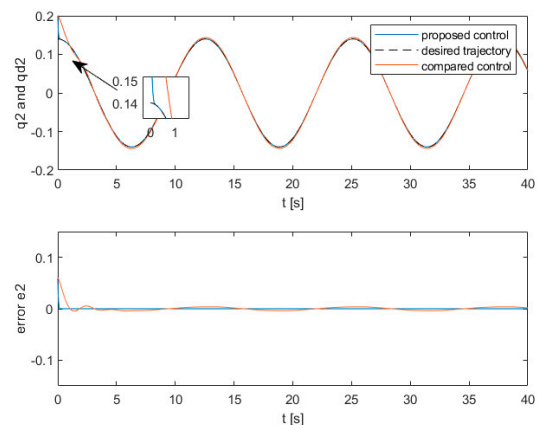


Figure 6. The trajectory tracking and error of joint 2.

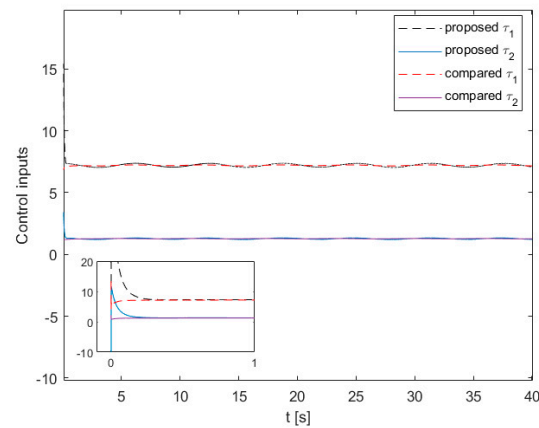


Figure 7. The proposed control inputs compared with the NSTSMC.

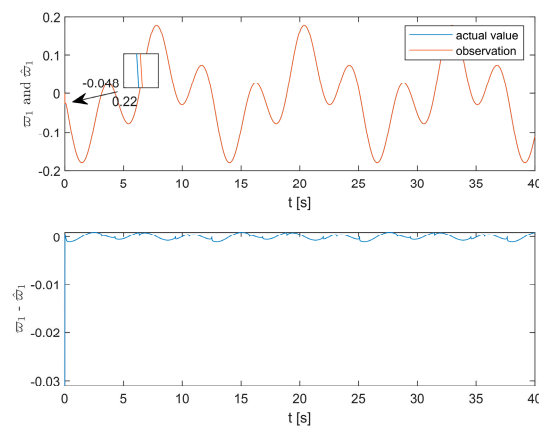


Figure 8. The observation effects of the disturbance observer—joint 1.

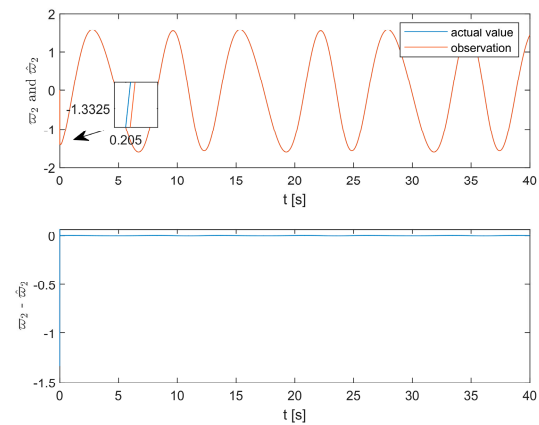


Figure 9. The observation effects of the disturbance observer—joint 2.

Additionally, both controllers successfully tracked the desired trajectory with favorable tracking response characteristics. Under both methods, the position error of the robotic arm achieved global time convergence. The convergence time of the NSTSMC was about 2.5 s, while the method in this article had a faster convergence speed of about 0.43 s, and the convergence time was less than the set time $\min(T_5) = 1.74$ s. This is 82.8% faster than the NSTSMC. This indicates the superior tracking performance of the proposed control method in tracking the desired trajectory. In Figure 7, the control inputs based on the proposed control method in this article and the NSTSMC are shown. The black and blue lines represent the proposed control inputs, while the red and purple lines represent

the compared control inputs. In the initial stage, the compared control inputs show less chattering than the proposed control inputs. When the system is stable, both control methods achieve stable control inputs. This indicates the robustness of the proposed control law with system uncertainties.

Figures 8 and 9 show the observation effects of the system uncertainties of joints 1 and 2, respectively, where ω_1 and $\hat{\omega}_1$ represent the actual value and observed value of ω of joint 1, respectively, and ω_2 and $\hat{\omega}_2$ represent the actual value and observed value of ω of joint 2, respectively. By analyzing Figures 8 and 9, it is evident that the designed disturbance observer can accurately estimate the system uncertainties present in the system, and real-time compensation can be performed on the control inputs, effectively enhancing the control precision and convergence speed of the system.

In summary, the above simulation results verify the correctness and effectiveness of the designed controller and disturbance observer.

6. Conclusions

In this article, a backstepping fixed-time control method based on disturbance observer compensation was proposed for an n-link robotic arm. The stability of the designed controller and observer was proven based on the Lyapunov theory, and accurate trajectory tracking of the robotic arm under system uncertainties was realized and, at the same time, ensuring that all signals in the closed-loop system are globally fixed-time-stable. Simulation verification showed that the control scheme proposed in this article achieved the desired response characteristics and tracking performance. The observer designed in this article also accurately estimated the system uncertainties, effectively improving the robustness of the system by continuously providing compensation to the controller. The method proposed in this article can also be used for other Euler–Lagrange systems, such as full-actuated ships or multiple-agent systems. Future work will consider adjusting the control parameters using optimal algorithms.

Author Contributions: Conceptualization, J.P.; data curation, J.P.; formal analysis, G.Z., J.P. and T.L.; funding acquisition, G.Z. and D.W.; investigation, T.L. and Z.W.; methodology, G.Z., J.P. and D.W.; software, J.P. and D.W.; supervision, G.Z. and Z.W.; validation, J.P.; writing—original draft, J.P.; writing—review and editing, G.Z., Z.W. and D.W. All authors have read and agreed to the published version of the manuscript.

Funding: This research was funded by the Startup Fund for Distinguished Scholars of West Anhui University under Grant No. WGKQ2022050 and the Smart Agriculture and Forestry and Smart Equipment Scientific Research and Innovation Team Anhui Undergrowth Crop Intelligent Equipment Engineering Research Center under Grant No. 2022AH010091.

Data Availability Statement: All data used to support the findings of this study are included within the article.

Acknowledgments: The authors would like to thank everyone involved for their contributions to this article. They would also like to thank the editors and anonymous reviewers for their helpful comments and suggestions.

Conflicts of Interest: The authors declare no conflicts of interest.

References

1. Zhou, J.; Li, Z.; Li, X.; Wang, X.; Song, R. Human–Robot Cooperation Control Based on Trajectory Deformation Algorithm for a Lower Limb Rehabilitation Robot. *IEEE/ASME Trans. Mechatron.* **2021**, *26*, 3128–3138. [[CrossRef](#)]
2. Cheng, L.W.; Li, D.L.; Yu, G.J.; Zhang, Z.H.; Yu, S.Y. Robotic arm control system based on brain-muscle mixed signals. *Biomed. Signal Process. Control* **2022**, *77*, 103754. [[CrossRef](#)]
3. Wu, Y.F.; Niu, W.K.; Kong, L.H.; Yu, X.B.; He, W. Fixed-time neural network control of a robotic manipulator with input deadzone. *ISA Trans.* **2023**, *135*, 449–461. [[CrossRef](#)] [[PubMed](#)]
4. González-Rodríguez, A.; Baray-Arana, R.E.; Rodríguez-Mata, A.E.; Robledo-Vega, I.; Acosta Cano de los Ríos, P.R. Validation of a Classical Sliding Mode Control Applied to a Physical Robotic Arm with Six Degrees of Freedom. *Processes* **2022**, *10*, 2699. [[CrossRef](#)]

5. Zhou, X.Y.; Wang, H.P.; Wu, K.; Zheng, G. Fixed-time neural network trajectory tracking control for the rigid-flexible coupled robotic mechanisms with large beam-deflections. *Appl. Math. Model.* **2023**, *118*, 665–691. [[CrossRef](#)]
6. Hernandez-Sanchez, A.; Chairez, I.; Matehuala-Moran, I.; Alfaro-Ponce, M.; Molina, A. Trajectory tracking controller of a robotized arm with joint constraints, a direct adaptive gain with state limitations approach. *ISA Trans.* **2023**, *141*, 276–287. [[CrossRef](#)] [[PubMed](#)]
7. Jia, Y.G.; Misra, A.K. Robust trajectory tracking control of a dual-arm space robot actuated by control moment gyroscopes. *Acta Astronaut.* **2017**, *137*, 287–301. [[CrossRef](#)]
8. Mai, T.L.; Tran, H.T. An adaptive robust backstepping improved control scheme for mobile manipulators robot. *ISA Trans.* **2023**, *137*, 446–456. [[CrossRef](#)]
9. Tuan, L.A.; Joo, Y.H.; Tien, L.Q.; Duong, P.X. Adaptive neural network second-order sliding mode control of dual arm robots. *Int. J. Control* **2017**, *15*, 2883–2891. [[CrossRef](#)]
10. Wang, H.; Liu, P.X.; Zhao, X.; Liu, X. Adaptive Fuzzy Finite-Time Control of Nonlinear Systems with Actuator Faults. *IEEE Trans. Cybern.* **2020**, *50*, 1786–1797. [[CrossRef](#)]
11. Dong, G.; Li, H.; Ma, H.; Lu, R. Finite-Time Consensus Tracking Neural Network FTC of Multi-Agent Systems. *IEEE Trans. Neural Netw. Learn. Syst.* **2021**, *32*, 653–662. [[CrossRef](#)] [[PubMed](#)]
12. Van, M.; Mavrovouniotis, M.; Ge, S.S. An Adaptive Backstepping Nonsingular Fast Terminal Sliding Mode Control for Robust Fault Tolerant Control of Robot Manipulators. *IEEE Trans. Syst. Man Cybern. Syst.* **2019**, *49*, 1448–1458. [[CrossRef](#)]
13. Yang, P.; Su, Y.X.; Zhang, L.Y. Proximate fixed-time fault-tolerant tracking control for robot manipulators with prescribed performance. *Automatica* **2023**, *157*, 111262. [[CrossRef](#)]
14. Shi, S.; Gu, J.; Xu, S.; Min, H. Globally Fixed-Time High-Order Sliding Mode Control for New Sliding Mode Systems Subject to Mismatched Terms and Its Application. *IEEE Trans. Ind. Electron.* **2020**, *67*, 10776–10786. [[CrossRef](#)]
15. Zhang, L.; Liu, H.; Tang, D.; Hou, Y.; Wang, Y. Adaptive Fixed Time Fault-Tolerant Tracking Control and Its Application for Robot Manipulators. *IEEE Trans. Ind. Electron.* **2021**, *69*, 2956–2966. [[CrossRef](#)]
16. Jin, X. Adaptive Fixed-Time Control for MIMO Nonlinear Systems With Asymmetric Output Constraints Using Universal Barrier Functions. *IEEE Trans. Autom. Control* **2019**, *64*, 3046–3053. [[CrossRef](#)]
17. Hua, C.; Ning, P.; Li, K.; Guan, X. Fixed-Time Prescribed Tracking Control for Stochastic Nonlinear Systems with Unknown Measurement Sensitivity. *IEEE Trans. Cybern.* **2022**, *52*, 3722–3732. [[CrossRef](#)]
18. Rahimi, S.; Jalali, H.; Mohammad, R.H.Y.; Kalhor, A.; Masouleh, M.T. Design and practical implementation of a Neural Network self-tuned Inverse Dynamic Controller for a 3-DoF Delta parallel robot based on Arc Length Function for smooth trajectory tracking. *Mechatronics* **2022**, *84*, 102772. [[CrossRef](#)]
19. Hu, J.B.; Zhang, D.; Wu, Z.G.; Li, H.Y. Neural network-based adaptive second-order sliding mode control for uncertain manipulator systems with input saturation. *ISA Trans.* **2023**, *136*, 126–138. [[CrossRef](#)]
20. Zhu, C.; Jiang, Y.; Yang, C. Fixed-Time Neural Control of Robot Manipulator With Global Stability and Guaranteed Transient Performance. *IEEE Trans. Ind. Electron.* **2023**, *70*, 803–812. [[CrossRef](#)]
21. Liang, X.L.; Wang, H.B.; Zhang, Y.X. Adaptive nonsingular terminal sliding mode control for rehabilitation robots. *Comput. Electr. Eng.* **2022**, *99*, 107718. [[CrossRef](#)]
22. Zhou, X.Y.; Wang, H.P.; Wu, K.; Tian, Y.; Zheng, G. Nonlinear disturbance observer-based robust predefined time tracking and vibration suppression control for the rigid-flexible coupled robotic mechanisms with large beam-deformations. *Comput. Math. Appl.* **2023**, *148*, 1–25. [[CrossRef](#)]
23. Yao, Q. Dual-disturbance-observer-based robust finite-time trajectory tracking control for robotic surface vehicle under measurement uncertainties. *Ocean. Eng.* **2021**, *242*, 110183. [[CrossRef](#)]
24. Ullah, I.; Pei, H.-L. Fixed Time Disturbance Observer Based Sliding Mode Control for a Miniature Unmanned Helicopter Hover Operations in Presence of External Disturbances. *IEEE Access* **2020**, *8*, 73173–73181. [[CrossRef](#)]
25. Vo, A.T.; Truong, T.N.; Kang, H.-J.; Van, M. A Robust Observer-Based Control Strategy for n-DOF Uncertain Robot Manipulators with Fixed-Time Stability. *Sensors* **2021**, *21*, 7084. [[CrossRef](#)] [[PubMed](#)]
26. Zou, Z.Y.; Tie, L. A new class of finite-time nonlinear consensus protocols for multi-agent systems. *Int. J. Control* **2014**, *87*, 363–370.
27. Fu, J.J.; Wang, J.Z. Fixed-time coordinated tracking for second-order multiagent systems with bounded input uncertainties. *Syst. Control Lett.* **2016**, *93*, 1–12. [[CrossRef](#)]
28. Su, B.; Wang, H.-b.; Wang, Y. Dynamic event-triggered formation control for AUVs with fixed-time integral sliding mode disturbance observer. *Ocean. Eng.* **2021**, *240*, 109893. [[CrossRef](#)]
29. Zuo, Z.Y. Nonsingular fixed-time consensus tracking for second-order multi-agent networks. *Automatica* **2015**, *54*, 305–309. [[CrossRef](#)]
30. He, W.; Ge, S.S.; Li, Y.; Chew, E.; Ng, Y.S. Neural Network Control of a Rehabilitation Robot by State and Output Feedback. *J. Intell. Robot. Syst.* **2015**, *80*, 15–31. [[CrossRef](#)]

Disclaimer/Publisher’s Note: The statements, opinions and data contained in all publications are solely those of the individual author(s) and contributor(s) and not of MDPI and/or the editor(s). MDPI and/or the editor(s) disclaim responsibility for any injury to people or property resulting from any ideas, methods, instructions or products referred to in the content.